CHAPTER 3

Broad-Scale Patterns of Forest Fire Occurrence Across the United States and the Caribbean Territories, 2022

Kevin M. Potter

INTRODUCTION

Wildland fire is an important natural component of many forest ecosystems that are characterized by specific combinations of fire frequency, severity, and seasonality (Greenberg and Collins 2021). It is a widespread disturbance agent in many U.S. forest ecosystems, causing widespread tree damage and mortality and impacting forest health both positively and negatively (Agee 1998, Thom and Seidl 2016, Wade and others 2000). In some ecosystems, wildland fire has been essential for regulating processes that maintain forest health (Lundquist and others 2011). For example, it is an important ecological mechanism that shapes the distributions of species, maintains the structure and function of fire-prone communities, and acts as a significant evolutionary force (Bond and Keeley 2005, Pausas and Keeley 2019). Additionally, some forest types and tree species are adapted to fire under certain intensities and return intervals (Hanberry and others 2018, Jeronimo and others 2019).

At the same time, wildland fires have created forest health and sustainability problems in some ecosystems (Edmonds and others 2011). Fires in some regions and ecosystems have become larger, more intense, and more damaging because of the accumulation of fuels from prolonged fire suppression and past management (Pyne 2010). Robust research indicates that climate change, via more common hot droughts, has already played a role in increased wildfire activity (Abatzoglou and Williams 2016, Higuera and Abatzoglou 2021). Current fire regimes on more than half the forested area in the conterminous United States (CONUS) have been moderately or significantly altered from historical regimes (Barbour and others 1999), potentially changing key ecosystem components, such as species composition, structural stage, stand age, canopy closure, and fuel loadings (Schmidt and others 2002, Stephens and others 2018). Evidence, in fact, suggests that few entirely natural fire regimes remain in North America (Parisien and others 2016). Such changes in fire intensity and recurrence could result in decreased forest resilience and persistence (Lundquist and others 2011), with plant communities in some regions undergoing rapid compositional and structural changes following fire suppression (Coop and others 2020, May and others 2023, Nowacki and Abrams 2008). Additionally, severe fires in combination with climate change are contributing to widespread challenges to natural regeneration, which threatens to lead to long-term conversions from forest to other vegetation types (Davis and others 2019, Stephens and others 2018).

In addition to their ecological and forest health consequences, large wildland fires also can have long-lasting social and economic consequences, including the loss of human life and property, smoke-related human health impacts, and the economic cost and dangers of fighting the fires themselves (Gill and others 2013, Richardson and others 2012). These impacts are particularly intense within the wildland-urban interface (the zone where human development mixes with forest), the area of which expanded 33 percent between 1990 and 2010 (Calkin and others 2015, Radeloff and others 2018). Additionally,

How to cite this chapter:

Potter, K.M. 2024. Broad-scale patterns of forest fire occurrence across the United States and the Caribbean territories, 2022. In: Pandit, K.; Conkling, B.L., eds. Forest Health Monitoring: national status, trends, and analysis 2023. Gen. Tech. Rep. WO-105. Washington, DC: U.S. Department of Agriculture, Forest Service: 57–85. Chapter 3. https://doi.org/10.2737/WO-GTR-105-Chap3.

exposure to wildfire smoke may have increased SARS-CoV-2 positivity rates among the public and thereby exacerbated the COVID-19 (coronavirus) pandemic (Kiser and others 2021).

This chapter presents analyses of daily satellite-based fire occurrence data that map and quantify the locations and intensities of fire occurrences spatially across the CONUS, Alaska, Hawaii, and the Caribbean territories in 2022. It also compares 2022 fire occurrences, within a geographic context, to all the recent years for which such data are available. Quantifying and monitoring such large-scale patterns of fire occurrence across the United States, as described in this chapter, cannot necessarily reveal whether the status and trends in wildland fire are "good" or "bad," but they can help improve understanding of the ecological and economic impacts of fire, including those associated with changing fire regimes across the United States. Additionally, large-scale assessments of fire occurrence can help identify areas where specific management activities may be needed, or where research into the ecological and socioeconomic impacts of fires would be beneficial.

METHODS

Data

The Moderate Resolution Imaging Spectroradiometer (MODIS) Rapid Response System (Justice and others 2002, 2011) extracts fire location and intensity information from the thermal infrared bands of imagery collected daily by two satellites at a resolution of 1 km, with the center of a pixel recorded as a fire occurrence (NASA Fire Information for Resource Management System 2022). The MODIS Active Fire Detections for the United States database (NASA Fire Information for Resource Management System 2023) allows analysts to spatially display and summarize fire occurrences across broad geographic regions for monitoring and reporting of wildland fire events (Coulston and others 2005; Potter 2012a, 2012b, 2013a, 2013b, 2014, 2015a, 2015b, 2016, 2017, 2018, 2019, 2020a, 2021, 2022, 2023). The MODIS sensors on the Terra and Aqua satellites identify the presence of a fire at the time of image collection by using a contextual algorithm that exploits the strong emission of mid-infrared radiation from fires (Giglio and others 2003). A fire occurrence is defined as one daily satellite detection of wildland fire in an approximately 1-km pixel, with multiple fire occurrences possible on a pixel across multiple days resulting from a single wildland fire that lasts more than 1 day. The resulting fire occurrence data represent only whether a fire was active because the MODIS data bands may not differentiate between a hot fire in a relatively small area (0.01 km^2, for example) and a cooler fire over a larger area (1 km^2, for example) if the foreground-to-background temperature contrast is not sufficiently high. The MODIS Active Fire database does well at capturing large fires during cloud-free conditions but may underrepresent rapidly burning, small, and low-intensity fires, as well as fires in areas with frequent cloud cover (Hawbaker and others 2008). The likelihood of detecting a fire beneath a tree canopy is probably low given the smaller general size of such fires and the fact that they are obscured by the canopy (Giglio and others 2018). For large-scale assessments, the dataset represents a good alternative to the use of ignition point information, which can be difficult to obtain or may not exist for many fires (Tonini and others 2009). The fire occurrence data additionally do not distinguish fires intentionally set for management purposes (controlled burns), which are common in some parts of the United States, such as the South, where many prescribed fires are smaller and/or lower severity and thus not detected by satellite sensors (Nowell and others 2018). More information about the performance of this product is provided by Justice and others (2011). For this analysis, standard MODIS fire occurrence data (those that are internally consistent and well calibrated following post-collection processing) were available from January 1 through September 30, 2022. Available data from October 1 through December 31 were near-real-time fire products, for which fire occurrence locations may not be as accurate, especially for the Aqua satellite, with errors typically small (<100 m) but sometimes larger (several kilometers) (NASA Fire Information for Resource Management System 2022).

Note that estimates of burned area (e.g., Monitoring Trends in Burn Severity data (Eidenshink and others 2007, Picotte and others 2020)) and calculations of MODIS-detected fire occurrences are different metrics for quantifying fire activity within a given year. Most importantly, the MODIS data contain both spatial and temporal components because persistent fire will be detected repeatedly over several days on a given 1-km pixel. In other words, a location can have a fire occurrence multiple times, once for each day a fire is detected at the location. Analyses of the MODIS-detected fire occurrences, therefore, measure the total number of daily 1-km pixels with fire during a year, as opposed to quantifying only the area on which fire occurred at some point during that timeframe. A fire detected on a single pixel every day for a week, for example, would be equivalent to seven fire occurrences.

The Terra and Aqua satellites that carry the MODIS sensors were launched in 1999 and 2002, respectively, and will be decommissioned eventually. An alternative fire occurrence data source is provided by the Visible Infrared Imaging Radiometer Suite (VIIRS) sensors on board the Suomi National Polar-orbiting Partnership (Suomi NPP) and NOAA-20 weather satellites. The transition to VIIRS 375-m data for national and regional fire occurrence monitoring will require a comparison of fire occurrence detections between it and MODIS. This is because science-ready VIIRS fire data are available only from 2015 onward (NASA Fire Information for Resource Management System 2022) compared to more than 20 years for the MODIS data. Ideally, assessments of fire occurrence trends would analyze as long a temporal window as possible (i.e., from near the beginning of MODIS data availability), encompassing the combination of older MODIS data with newer VIIRS data.

Analyses

Using ArcMap® (ESRI 2017), these MODIS products were processed for 2022 and for the 21 preceding full years of data (beginning in 2001 because of issues with data collection and processing from the Terra satellite in 2000). This determined forest fire occurrence density for (1) ecoregion sections in the CONUS (Cleland and others 2007), (2) ecoregions on each of the major islands of Hawaii (Potter 2020b), and (3) the islands of the Caribbean territories of Puerto Rico and the U.S. Virgin Islands. Fire occurrence density was defined as the number of fire occurrences per 100 km^2 (10 000 ha) of tree canopy cover area. Forest fire occurrence density metrics were calculated for the CONUS, Hawaii, and the Caribbean territories for each year after screening out wildland fires that did not intersect with tree canopy data. The tree canopy data had been resampled to 240 m from a 30-m raster dataset that estimates percentage of tree canopy cover (from 0 to 100 percent) for each grid cell. This dataset was generated from the 2011 National Land Cover Database (NLCD) (Homer and others 2015) through a cooperative project between the Multi-Resolution Land Characteristics Consortium and the U.S. Department of Agriculture, Forest Service, Geospatial Technology and Applications Center (GTAC) (Coulston and others 2012). For the purposes of this study, any cell with >0 percent tree canopy cover was treated as forest. (This would not include shrub and chapparal land cover without trees.) Comparable tree canopy cover data were not available for Alaska, so a 240-m-resolution layer of forest and shrub cover was instead created from the 2011 NLCD. The MODIS fire occurrence detection data was then intersected with this layer and with ecoregion sections (Spencer and others 2002) to calculate the number of fire occurrences per 100 km^2 of forest and shrub cover within each ecoregion section in Alaska. Separately determined were the total numbers of forest fire occurrences for the CONUS, Alaska, Hawaii, and the Caribbean territories after clipping the MODIS fire occurrences by the tree canopy cover or tree and shrub cover data.

The fire occurrence density value for each of the ecoregions of the States and for the Caribbean territories in 2022 was compared with the mean fire density values for the first 21 full years of MODIS Active Fire data collection (2001–2021). Specifically, the difference of the 2022 value and the previous 21-year mean for the area was divided by the standard deviation across the previous 21-year period, assuming a normal distribution of fire density over time. The result for each ecoregion was a standardized z-score, which is a dimensionless quantity describing the degree to which the fire occurrence density in the area in 2022 was higher, lower, or the same relative to all the previous years for which data have been collected, accounting for the variability in the previous years. The z-score is the number of standard deviations between the observation and the mean of the historic observations in the previous years. Approximately 68 percent of observations would be expected within one standard deviation of the mean, and 95 percent within two standard deviations. Near-normal conditions are those within a single standard deviation of the mean, although such a threshold is somewhat arbitrary. Conditions between about one and two standard deviations of the mean are moderately different from mean conditions but are not significantly different statistically. Those outside about two standard deviations would be considered statistically greater than or less than the long-term mean (p <0.025 at each tail of the distribution).

Additionally, the Spatial Association of Scalable Hexagons (SASH) analytical approach identified forested areas in the CONUS with higher-than-expected fire occurrence density in 2022. This method identifies locations where ecological phenomena occur at greater or lower occurrences than expected by random chance and is based on a sampling frame optimized for spatial neighborhood analysis, adjustable to the appropriate spatial resolution, and applicable to multiple data types (Potter and others 2016). Specifically, it consists of dividing an analysis area into scalable equal-area hexagonal cells within which data are aggregated, followed by identifying statistically significant geographic clusters of hexagonal cells within which mean values are greater or less than those expected by chance. These clusters were identified through a Getis-Ord G_i^* hotspot analysis (Getis and Ord 1992) in ArcMap® 10.5.1 (ESRI 2017).

The spatial units of analysis were 9,810 hexagonal cells, each approximately 834 km^2 in area, generated in a lattice across the CONUS using intensification of the Environmental Monitoring and Assessment Program (EMAP) North American hexagon coordinates (White and others 1992). These coordinates are the foundation of a sampling frame in which a hexagonal lattice was projected onto the CONUS by centering a large base hexagon over the region (Reams and others 2005, White and others 1992). The hexagons are compact and uniform in their distance to the centroids of neighboring hexagons, meaning that a hexagonal lattice has a higher degree of isotropy (uniformity in all directions) than does a square grid (Shima and others 2010). These attributes are highly useful for spatial neighborhood analyses. Importantly, these scalable hexagons also are independent of geopolitical and ecological boundaries, avoiding the possibility of different sample units (such as counties, States, or watersheds) encompassing vastly different areas (Potter and others 2016). The 834-km^2 hexagons are a manageable size for making monitoring and management decisions in analyses across the CONUS (Potter and others 2016).

Fire occurrence density values were calculated as the number of forest fire occurrences per 100 km^2 of tree canopy cover area within a hexagon. Use of the Getis-Ord G_i^* statistic identified clusters of hexagonal cells with fire occurrence density values higher than expected by chance. This statistic allows for the decomposition of a global measure of spatial association into its contributing factors, by location, and is therefore particularly suitable for detecting outlier assemblages of similar conditions in a dataset, such as when spatial clustering is concentrated in one subregion of the data (Anselin 1992).

Briefly, G_i^* sums the differences between the mean values in a local sample, determined in this case by a moving window of each hexagon and its 18 first- and second-order neighbors (the 6 adjacent hexagons and the 12 additional hexagons contiguous to those 6) and the global mean of the 9,644 hexagonal cells with tree canopy cover (of the total 9,810) in the CONUS. As described in Laffan (2006), it is calculated as:

$$G_i^{*}(\boldsymbol{d}) = \frac{\sum_j w_{ij}(\boldsymbol{d})x_j - W_i^*\bar{x}^*}{s^*\sqrt{\frac{(ns_{1i}^*) - W_i^{*2}}{n-1}}}$$

where

G_i^* = the local clustering statistic (in this case, for the target hexagon)

i = the center of local neighborhood (the target hexagon)

d = the width of local sample window (the target hexagon and its first- and second-order neighbors)

x_j = the value of neighbor j

w_{ij} = the weight of neighbor j from location i (all the neighboring hexagons in the moving window were given an equal weight of 1)

n = the number of samples in the dataset (the 9,644 hexagons containing >5-percent tree cover and with at least 1 percent of the canopy cover surveyed)

W_i^* = the sum of the weights

s^*_{1i} = the number of samples within d of the central location (19: the focal hexagon and its 18 first- and second-order neighbors)

$\bar{x}^*$ = mean of whole dataset (in this case, the 9,644 hexagons)

s^* = the standard deviation of whole dataset (for the 9,644 hexagons)

G_i^* is standardized as a z-score with a mean of 0 and a standard deviation of 1, with values >1.96 representing significant local clustering of higher fire occurrence densities (p <0.025) and values <-1.96 representing significant clustering of lower fire occurrence densities (p <0.025), because 95 percent of the observations under a normal distribution should be within approximately two standard deviations of the mean (Laffan 2006). Values between -1.96 and 1.96 have no statistically significant concentration of high or low values. In other words, a hexagon and its 18 neighbors have a normal range of both high and low numbers of fire occurrences per 100 km^2 of tree canopy cover area. The threshold values are not exact because the correlation of spatial data violates the assumption of independence required for statistical significance (Laffan 2006). In addition, the Getis-Ord approach does not require that the input data be normally distributed, because the local G_i^* values are computed under a randomization assumption, with G_i^* equating to a standardized z-score that asymptotically tends to a normal distribution (Anselin 1992). The z-scores are reliable, even with skewed data, as long as the local neighborhood encompasses several observations (ESRI 2017): in this case, via the target hexagon and its 18 first- and second-order neighbors.

RESULTS AND DISCUSSION

Trends in Forest Fire Occurrence Detections for 2022

Across the CONUS, 62,297 forest fire occurrences were recorded in the MODIS Active Fire database for 2022. This represented a 44-percent decrease in fire activity from 2021 (111,416 fire occurrences) and was the 13th largest number of fire occurrences in 22 full years of data collection (fig. 3.1). It was also 17 percent less than the mean for the previous 21 years of data (74,753 fire occurrences). Meanwhile, Alaska experienced a >1,000-percent increase in forest fire occurrences in 2022 (21,320) compared to the previous year (1,806). The 2022 number was a 139 percent increase over the 21-year average of 8,931. It was the fifth highest number of fire occurrences in Alaska since the first full year of data collection in 2001 and repeated a trend of large fire years every few years for the State, last experienced in 2015 and 2019. Also, like 2019, the large Alaskan fire year in 2022 corresponded with a milder-than-average fire year for the CONUS. Additionally in 2022, 46 fire occurrences were detected in the State of Hawaii, a slight increase of 7 percent from 43 in 2021 but still 82 percent below the 2001–2021 average of about 262 a year. Finally, Puerto Rico and the U.S. Virgin Islands experienced 5 fire occurrences, which was a 62-percent decrease from 13 in 2021 and 45 percent below the average of about 9 per year.

These results do not correspond closely with official national wildland fire statistics tracking the number of wildfires reported and the area burned by them (National Interagency Coordination Center 2023). Nationally, the area burned increased about 6 percent from 2 883 645 ha in 20021 to 3 066 377 in 2022, and the number of individual wildfires reported climbed from 58,985 to 68,988 with higher increase in Alaska and the South (National Interagency Coordination Center 2023). The National Interagency Coordination Center uses a benchmark threshold of 16 187 ha (40,000 acres) for tracking very large wildland fires and fire complexes. More fires in 2022 (45) exceeded this threshold area than in 2021 (38), but this was fewer than the number in 2020 (50) (National Interagency Coordination Center 2021, 2022, 2023). Of these 45 very large fires in 2022, 30 were in Alaska. As noted above in Methods, the number of reported fires and estimates of burned area are different metrics for quantifying fire activity than are calculations of MODIS-detected fire occurrences, but the metrics may be correlated. The analyses described in this chapter focus on MODIS fire occurrences because they capture both the spatial and temporal components of persistent fires that are detected repeatedly over 2 or more days on a 1-km pixel, rather than quantifying only the area on which fire occurred.

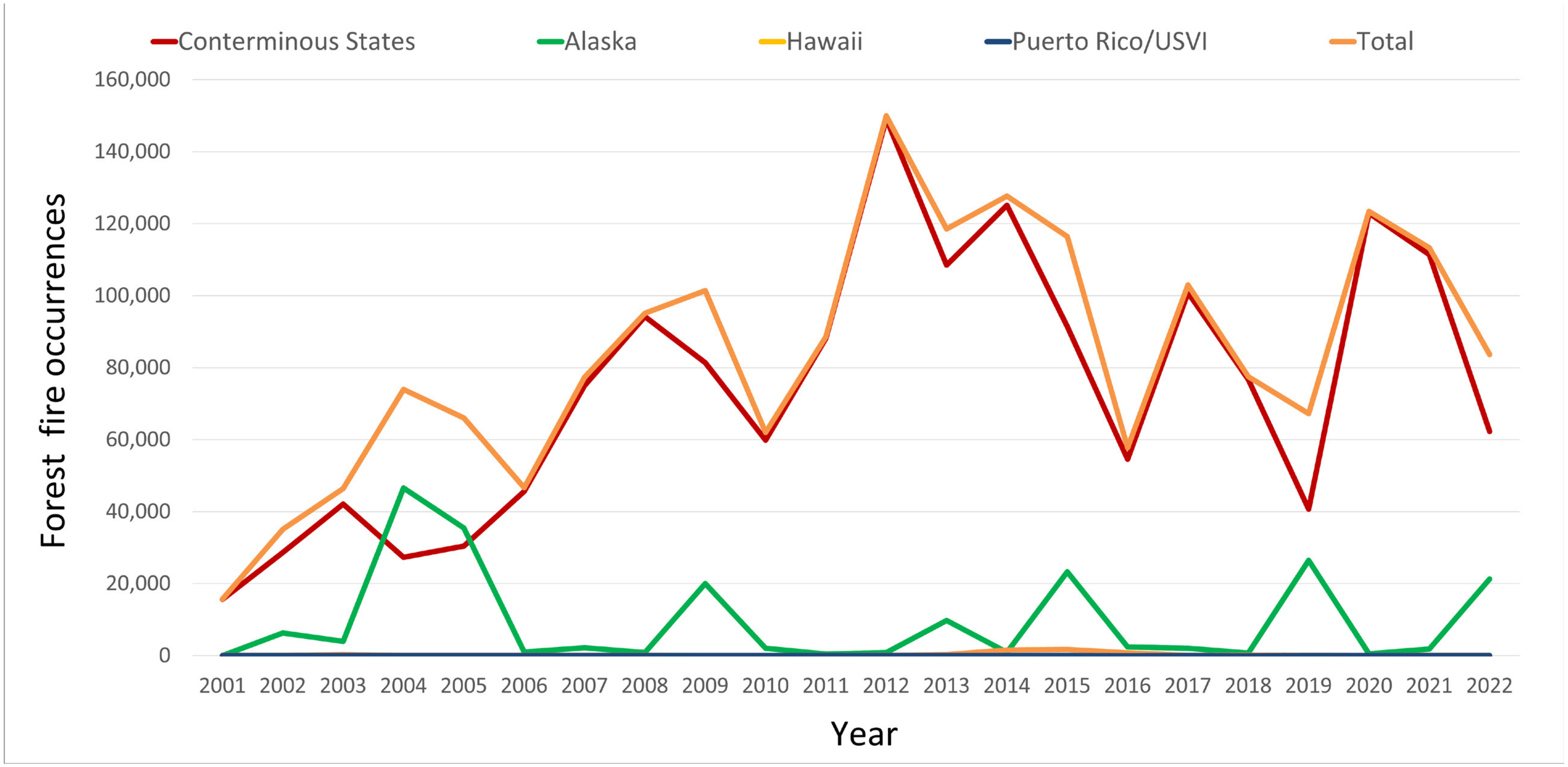

Figure 3.1—Forest fire occurrences detected by Moderate Resolution Imaging Spectroradiometer (MODIS) from 2001 through 2022 for the conterminous United States, Alaska, Hawaii, and Puerto Rico and the U.S. Virgin Islands, and for the entire Nation combined. (Data source: U.S. Department of Agriculture, Forest Service, Geospatial Technology and Applications Center, in conjunction with the NASA MODIS Rapid Response group)

The 2022 MODIS wildland fire occurrence data indicate that the areas with the highest fire occurrence densities shifted from recent years. In 2020 and 2021 (Potter 2022, 2023), ecoregions with extremely high fire occurrence densities were located in the northwestern and Sierra Nevada regions of California and in central Oregon and Washington. In 2022, no ecoregion sections had extremely high fire occurrence densities, but a handful in the Southwest had very high values (fig. 3.2). These were 315H–Central Rio Grande Intermontane in central New Mexico (20.8 fire occurrences/100 km^2 of tree canopy cover), M331F–Southern Parks and Rocky Mountain Range in north-central New Mexico and south-central Colorado (18.4 fire occurrences), and M313A–White Mountains-San Francisco Peaks-Mogollon Rim in southwestern New Mexico and east-central Arizona (17.2 fire occurrences) (table 3.1). (Note that the ecoregion section in 2021 with the highest fire occurrence density had 52.2 fire occurrences/100 km^2 of tree canopy cover (Potter 2023).) Many of the fires in this region were sparked by dry and frequently windy spring conditions that resulted in several long-duration fires, including the Hermits Peak and Black Fires in New Mexico, by the end of May (National Interagency Coordination Center 2023).

Other ecoregion sections with relatively high fire occurrence densities were located in the Pacific Northwest (M332A–Idaho Batholith, with 10.0 fire occurrences/100 km^2 of tree canopy cover, and M242D–Northern Cascades, 7.0 fire occurrences), central California (262A–Great Valley, 9.0 fire occurrences), and the Gulf Coast region (232B–Gulf Coastal Plains and Flatwoods, 6.0 fire occurrences).

Alaska, meanwhile, experienced well-above normal temperatures through the early summer of 2022. This was coupled with lightning-intense storms in the southwestern and interior parts of the State that generated a rapid increase in fire activity in June, with dozens of large fires burning by the end of that month (National Interagency Coordination Center 2023). As a result, a swath of ecoregion sections from southwestern to east-central Alaska had high fire occurrence densities: M133A–Lime Hills (10.2), M132B–Kuskokwim Mountains (9.3), and 132C–Tanana-Kuskokwim Lowlands (6.2) (fig. 3.3). The fire activity in Alaska began to wane in July with the spread of cooler and wetter conditions across the State (National Interagency Coordination Center 2023).

Hawaii ecoregions had relatively low fire occurrence densities in 2022. Only three exceeded 1 fire occurrence/100 km^2 of canopy cover: the Mesic ecological region on Hawai‘i Island (MEh, 2.1) and the Montane Wet-Maui-West (MWm-w, 1.7) and Mesic-Maui-West (MEm-w, 1.6) on Maui (fig. 3.4). At the same time, fire occurrence densities in 2022 were ≤1 fire occurrence/100 km^2 of tree canopy cover for most islands of the U.S. Caribbean territories (Puerto Rico and the U.S. Virgin Islands) except for Great Hans Lollik Island north of Saint Thomas in the U.S. Virgin Islands (72.9), which is quite small and had a single fire occurrence (fig. 3.5).

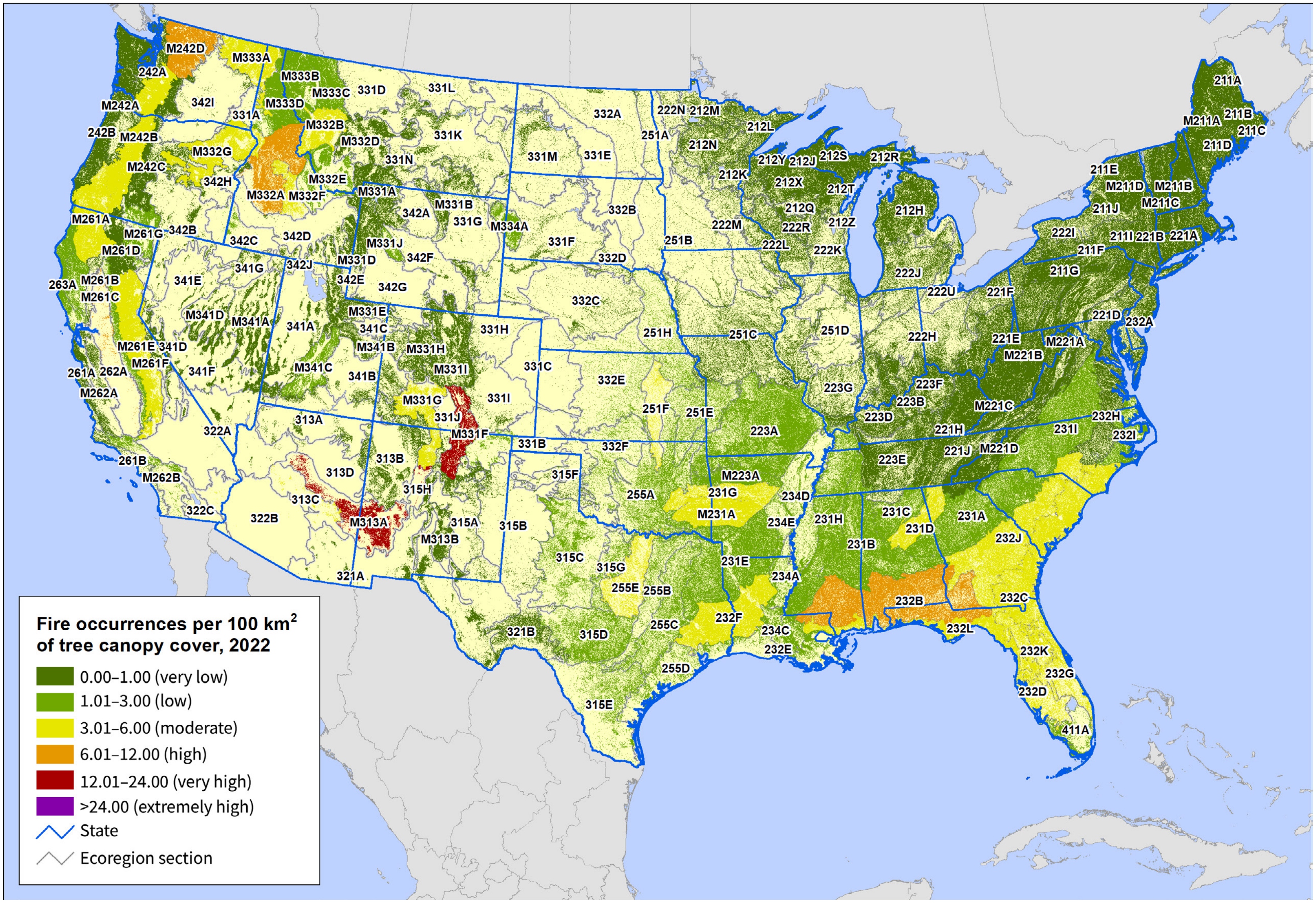

Figure 3.2—The number of forest fire occurrences per 100 km² (10 000 ha) of tree canopy coverage area, by ecoregion section within the conterminous United States, for 2022. The gray lines delineate ecoregion sections (Cleland and others 2007). Tree canopy cover is based on data from a cooperative project between the Multi-Resolution Land Characteristics Consortium (Coulston and others 2012) and the Forest Service Geospatial Technology and Applications Center (GTAC) using the 2011 National Land Cover Database. See figure 1.1A for ecoregion identification. (Source of fire data: U.S. Department of Agriculture, Forest Service, GTAC, in conjunction with the NASA Moderate Resolution Imaging Spectroradiometer Rapid Response group)

Table 3.1—The 15 ecoregion sections in the conterminous United States with the highest fire occurrence densities in 2022

Section	Name	Tree canopy area (100 km^2)	Fire occurrences (number)	Density[a]
315H	Central Rio Grande Intermontane	7.1	147	20.8
M331F	Southern Parks and Rocky Mountain Range	174.7	3,221	18.4
M313A	White Mountains-San Francisco Peaks-Mogollon Rim	202.5	3,476	17.2
M332A	Idaho Batholith	338.9	3,393	10.0
262A	Great Valley	19.4	176	9.0
M242D	Northern Cascades	251.1	1,763	7.0
232B	Gulf Coastal Plains and Flatwoods	888.7	5,355	6.0
232J	Southern Atlantic Coastal Plains and Flatwoods	604.0	3,588	5.9
M261E	Sierra Nevada	427.8	2,473	5.8
M332G	Blue Mountains	309.7	1,728	5.6
322B	Sonoran Desert	2.2	12	5.5
M332F	Challis Volcanics	72.2	374	5.2
251F	Flint Hills	57.8	286	4.9
232K	Florida Coastal Plains Central Highlands	149.0	669	4.5
M331G	South-Central Highlands	187.5	824	4.4

[a] Density = fire occurrences per 100 km^2 of tree canopy coverage area.

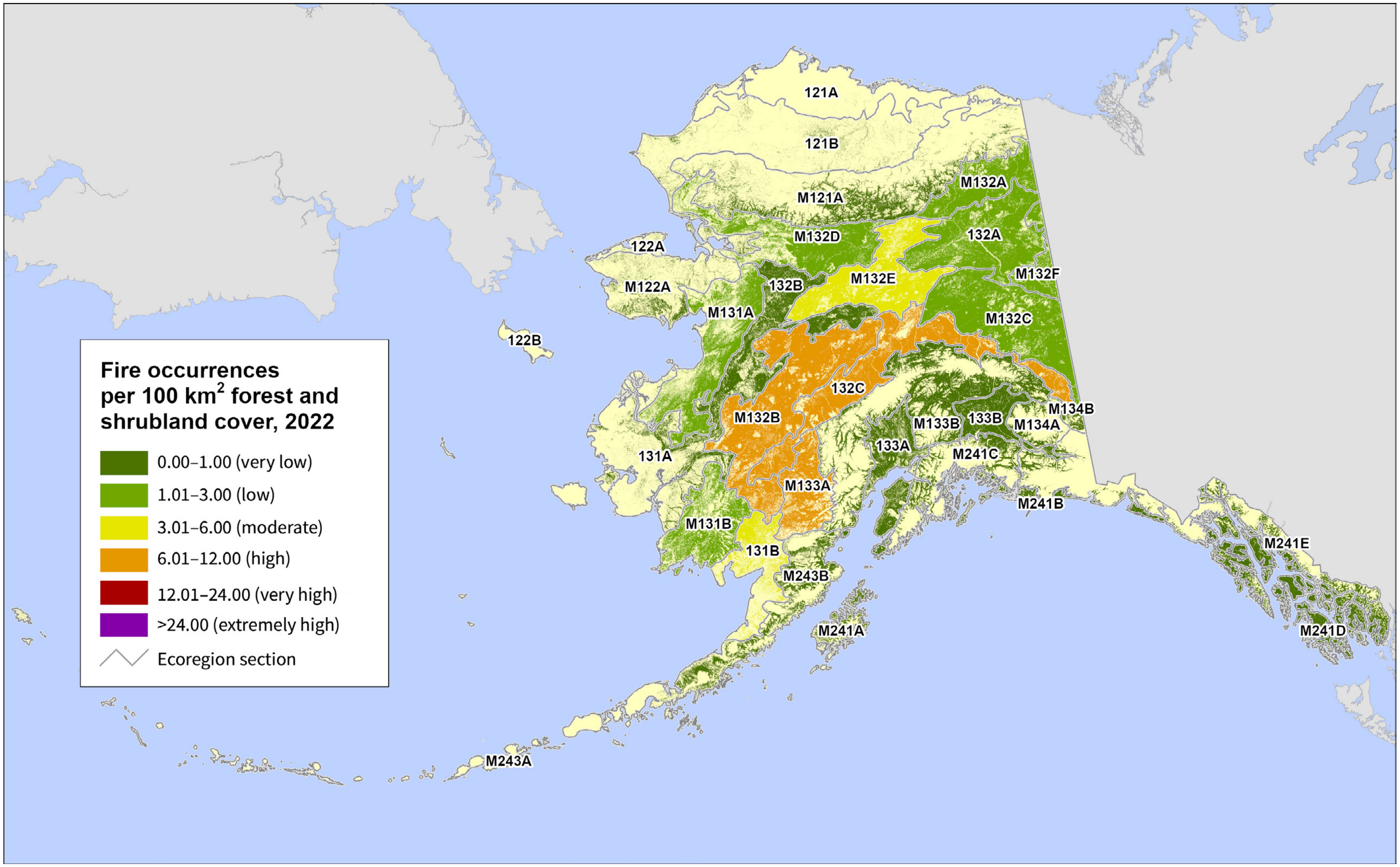

Figure 3.3—The number of forest fire occurrences per 100 km^2 (10 000 ha) of forest and shrub cover, by ecoregion section within Alaska, for 2022. The gray lines delineate ecoregion sections (Spencer and others 2002). Forest and shrub cover are derived from the 2011 National Land Cover Database. See figure 1.1B for ecoregion identification. (Source of fire data: U.S. Department of Agriculture, Forest Service, Geospatial Technology and Applications Center, in conjunction with the NASA Moderate Resolution Imaging Spectroradiometer Rapid Response group)

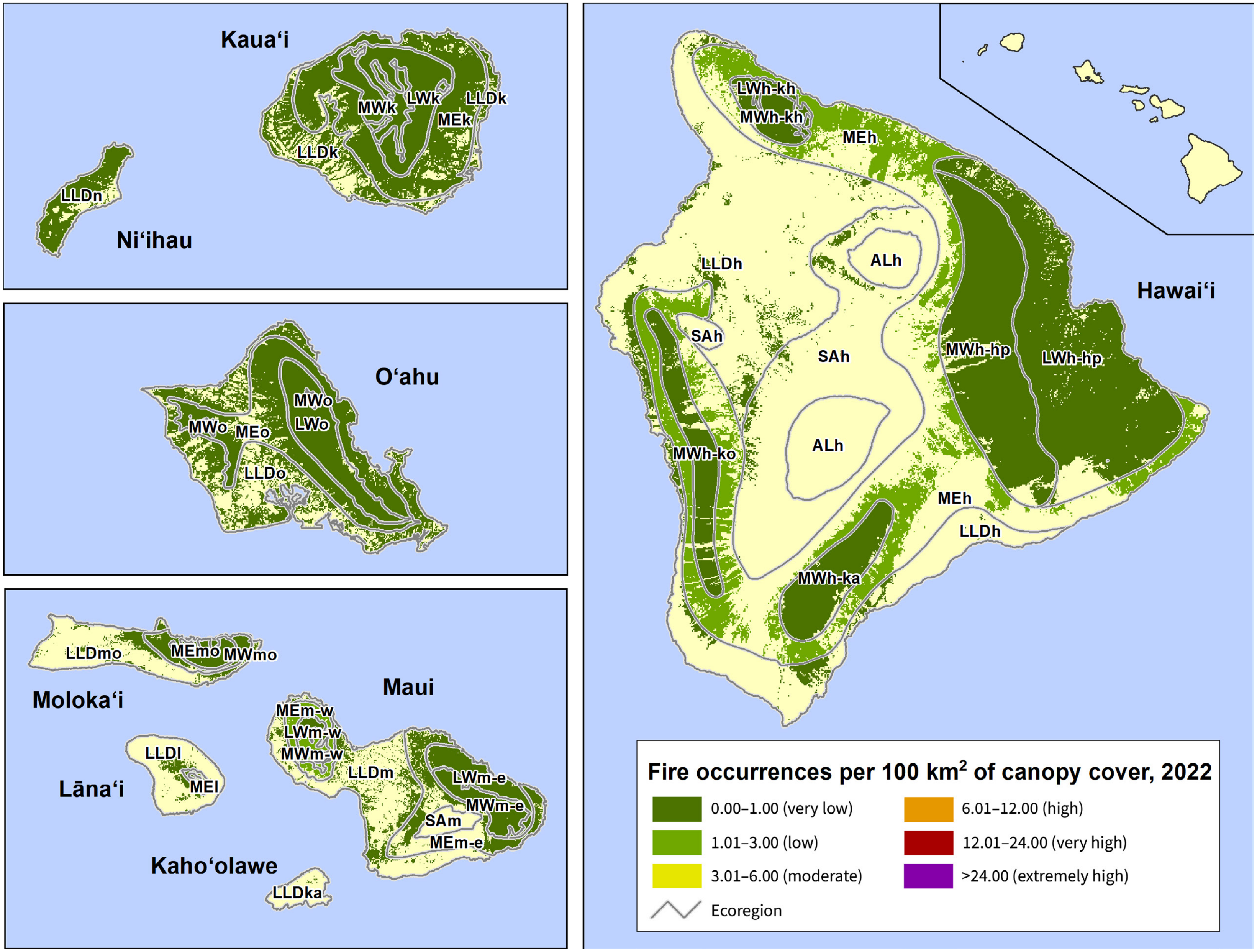

Figure 3.4—The number of forest fire occurrences per 100 km² (10 000 ha) of tree canopy coverage area, by island/ecoregion combination in Hawaii, for 2022. Tree canopy cover is based on data from a cooperative project between the Multi-Resolution Land Characteristics Consortium (Coulston and others 2012) and the Forest Service Geospatial Technology and Applications Center (GTAC) using the 2011 National Land Cover Database. (Source of fire data: U.S. Department of Agriculture, Forest Service, GTAC, in conjunction with the NASA Moderate Resolution Imaging Spectroradiometer Rapid Response group)

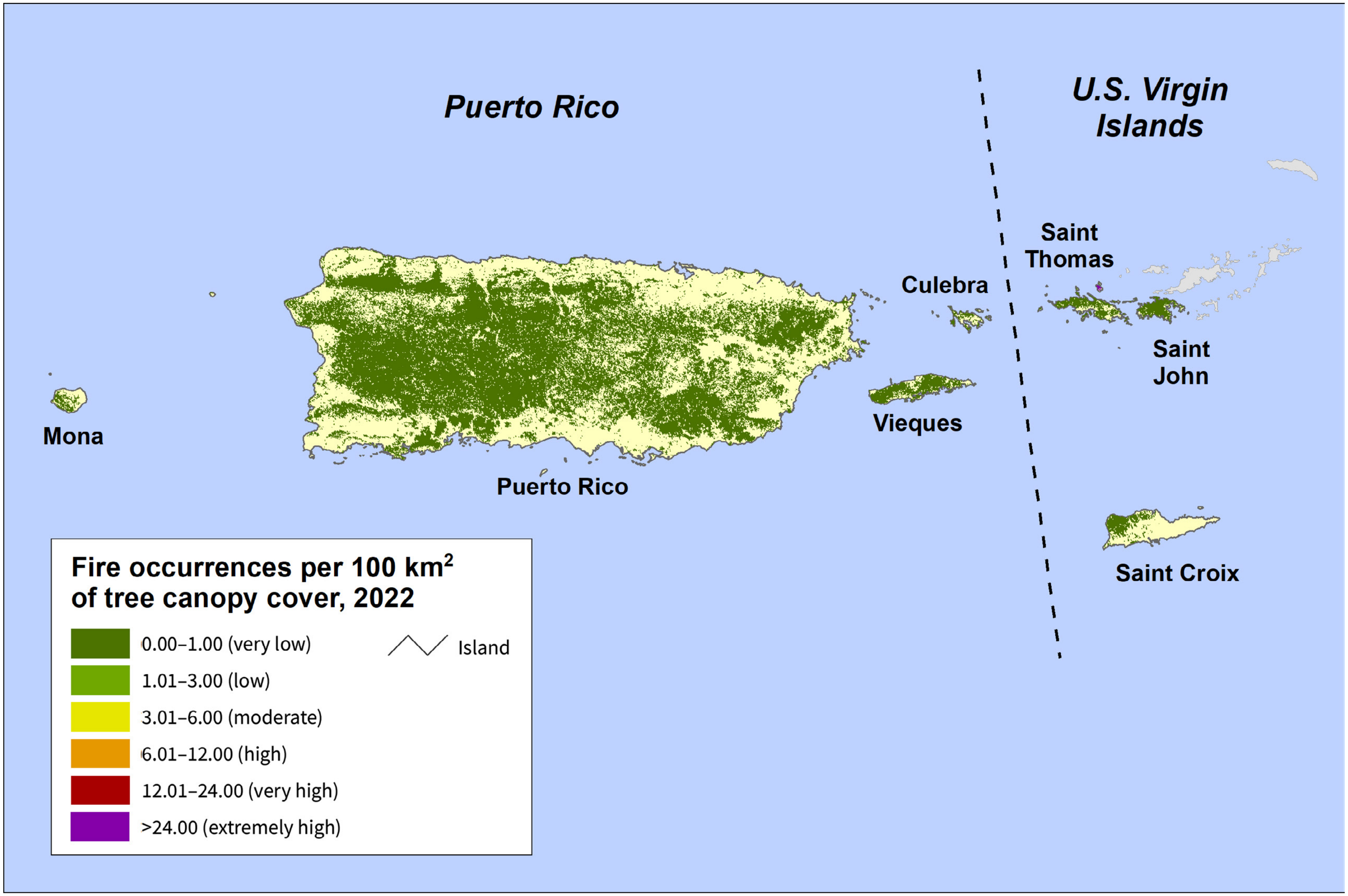

Figure 3.5—The number of forest fire occurrences per 100 km² (10 000 ha) of tree canopy coverage area, by island in Puerto Rico and the U.S. Virgin Islands, for 2022. Tree canopy cover is based on data from a cooperative project between the Multi-Resolution Land Characteristics Consortium (Coulston and others 2012) and the Forest Service Geospatial Technology and Applications Center (GTAC) using the 2011 National Land Cover Database. (Source of fire data: U.S. Department of Agriculture, Forest Service, GTAC, in conjunction with the NASA Moderate Resolution Imaging Spectroradiometer Rapid Response group)

Comparison to Longer Term Trends

The collection of MODIS Active Fire data for more than two decades allows one to contrast annual (2022) forest fire occurrence densities with longer term trends (2001–2021) for ecoregions in the CONUS, Alaska, and Hawaii, and for the Caribbean territories. During that 21-year comparison period, ecoregions in the Pacific Coast States, Idaho, Arizona/New Mexico, eastern Kansas/northeastern Oklahoma, and along the Gulf Coast in the Southeast had high mean annual fire occurrence densities (exceeding 6 fire occurrences/100 km^2 of tree canopy cover) (fig. 3.6A). The two specific ecoregion sections with the highest mean annual fire occurrence density (12.0 fire occurrences/100 km^2 of tree canopy cover annually) were M261A–Klamath Mountains of northwestern California and southeastern Oregon and M261B–Northern California Coast Ranges (table 3.2). Other ecoregion sections with high mean annual fire occurrence densities included M332A–Idaho Batholith in central Idaho (11.7), M261E–Sierra Nevada in California (11.4), and M262B–Southern California Mountain and Valley near the southern California coast (9.3). Several ecoregions in the West and Southeast had moderate mean fire occurrence densities (3–6 fire occurrences/100 km^2 of tree canopy cover annually), while much of the Midwest and all the Northeast had very low densities (≤1).

Many of the western ecoregion sections with the highest mean annual forest fire occurrence densities also had the greatest annual variation in fire occurrence densities from 2001 through 2021 (fig. 3.6B). This included M261B–Northern California Coast Ranges, M332A–Idaho Batholith, 261A–Central California Coast, M261E–Sierra Nevada, and M262B–Southern California Mountain and Valley. More moderate variation existed in other parts of the West, including central Oregon and Washington, northwestern Montana, and central Arizona and west-central New Mexico. Other areas—including in north-central Colorado and south-central Wyoming—had moderate variation with low mean annual fire occurrence densities, suggesting low numbers of fire occurrences most years with high numbers in others. Ecoregion sections of the Midwest and Northeast and in coastal Oregon and Washington had the lowest interannual variation (standard deviation <1), while slightly higher variation (standard deviation 1–5) was apparent across the Southeast, the central Rocky Mountains, and the Great Basin. Parts of the Southeast, especially along the Gulf Coast, had low annual variation but relatively high mean annual fire occurrence densities, indicating consistently high numbers of fire occurrences over time.

Compared to the previous 21-year mean and accounting for temporal variability, a handful of ecoregions in the Southwest, the Northeast, the Midwest, and the Mid-Atlantic States experienced 2022 fire occurrence densities that were higher than normal (fig. 3.6C). With *z*-scores >2, M331F–Southern Parks and Rocky Mountain Range, 315H–Central Rio Grande Intermontane, and 331B–Southern High Plains in the Southwest all had much higher 2022 fire occurrence densities than expected. The same was true of two ecoregion sections in Maine (211A–

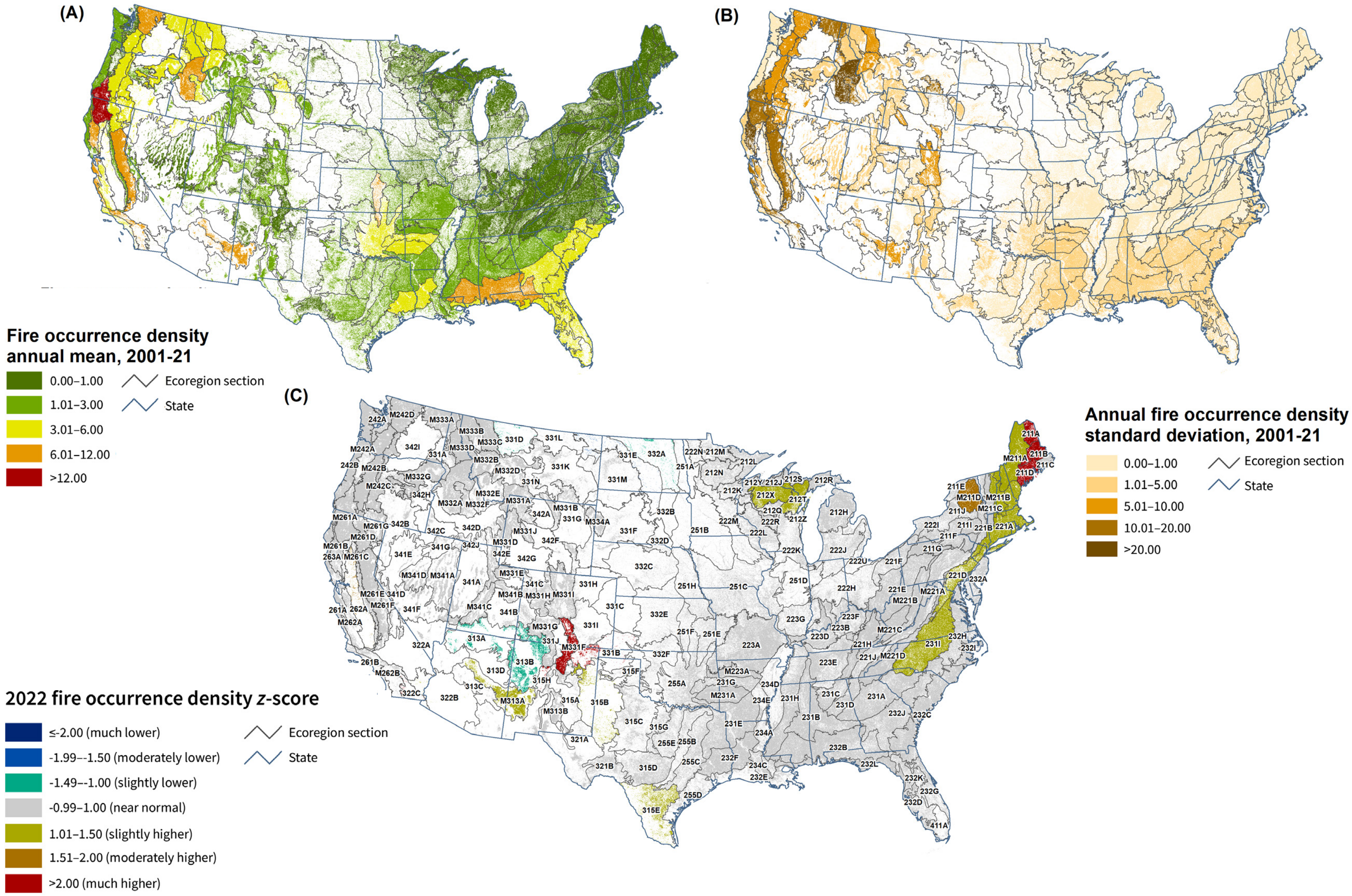

Figure 3.6—(A) Mean number and (B) standard deviation of forest fire occurrences per 100 km² (10 000 ha) of tree canopy coverage area from 2001 through 2021, by ecoregion section within the conterminous United States. (C) Degree of 2022 fire occurrence density excess or deficiency, by ecoregion section relative to 2001–2021 and accounting for variation over that period. The gray lines delineate ecoregion sections (Cleland and others 2007). Tree canopy cover is based on data from a cooperative project between the Multi-Resolution Land Characteristics Consortium (Coulston and others 2012) and the Forest Service Geospatial Technology and Applications Center (GTAC) using the 2011 National Land Cover Database. (Source of fire data: U.S. Department of Agriculture, Forest Service, GTAC, in conjunction with the NASA Moderate Resolution Imaging Spectroradiometer Rapid Response group)

Table 3.2—The 15 ecoregion sections in the conterminous United States with the highest mean annual fire occurrence densities from 2001 through 2021

Section	Name	Tree canopy area (100 km^2)	Mean annual fire occurrence density[a]
M261A	Klamath Mountains	338.5	12.0
M261B	Northern California Coast Ranges	114.1	12.0
M332A	Idaho Batholith	338.9	11.7
M261E	Sierra Nevada	427.8	11.4
M262B	Southern California Mountain and Valley	58.1	9.3
M313A	White Mountains-San Francisco Peaks-Mogollon Rim	202.5	7.4
313C	Tonto Transition	17.5	7.2
251F	Flint Hills	57.8	6.9
261A	Central California Coast	66.8	6.7
M242D	Northern Cascades	251.1	6.4
232B	Gulf Coastal Plains and Flatwoods	888.7	6.1
M261D	Southern Cascades	150.6	5.9
M242C	Eastern Cascades	219.4	5.8
331A	Palouse Prairie	33.4	5.8
M332F	Challis Volcanics	72.2	5.5

[a] Mean annual fire occurrence density = fire occurrences per 100 km^2 of tree canopy coverage area.

Aroostook Hills and Lowlands and 211B–Maine-New Brunswick Foothills and Lowlands), though this was an area that did not have nearly as many fire occurrences in 2022 as the southwestern regions. In other words, these are areas that tend to have few fires in a typical year and therefore don't require many fire occurrences to be classified as having more than normal. Worth noting is the 2022 absence of areas with higher-than-normal fire occurrence densities in the Pacific Coast States; several ecoregions there experienced fire occurrence densities that were much higher than normal in both 2020 and 2021 (Potter 2022, 2023).

Meanwhile, a handful of ecoregion sections in the Upper Midwest and the Southwest had lower-than-expected fire occurrence densities in 2022, as indicated by z-scores ≤-1. This included 313A–Grand Canyon in northern Arizona and southern Utah, 313B–Navajo Canyonlands in northwestern New Mexico, 332A– Northeastern Glaciated Plains in central North Dakota, and 331D–Northwestern Glaciated Plains in north-central Montana. These are all areas with low to moderate annual fire occurrence densities on average.

Mean annual fire occurrence densities in Alaska for 2001–2021 were moderately high (3.0–6.0 fire occurrences/100 km^2 of tree canopy cover annually) in M132E–Ray Mountains and 132A–Yukon-Old Crow Basin of the State's central and east-central interior (fig. 3.7A). Most of the interior ecoregions around these had slightly lower mean annual fire occurrence densities, while those of northern, western, and southern Alaska (including the panhandle) were very low (≤1). Central and east-central interior ecoregions exhibited moderately high variability during the 21-year period preceding 2022 (fig. 3.7B). For that year, many Alaskan ecoregions had fire occurrence densities that were much higher or moderately higher than expected compared to the previous 21 years and controlling for variability, including in the southwestern, west-central, panhandle, and far northern parts of the State (fig. 3.7C). In southwestern Alaska, the massive 350 306-ha Lime Complex of fires spanned three ecoregion sections: M133A–Lime Hills, 132C–Tanana-Kuskokwim Lowlands, and M132B–Kuskokwim Mountains. In west-central Alaska, the 111 573-ha Paradise Complex, the 92 851-ha Tatlawiksuk Fire, and the 85 997-ha Bean Complex all extended across parts of M132B–Kuskokwim Mountains and 132C–Tanana-Kuskokwim Lowlands. The number of fire occurrences was relatively small in M121A–Brooks Range of the far north and M241D–Alexander Archipelago of the panhandle, but these areas still had much higher fire occurrence density than expected because they are areas that have very few fire occurrences on average.

For Hawaii, an ecological region on the eastern side of Hawai'i Island (Lowland Wet-Hilo-Puna (LWh-hp)) exhibited both the highest annual fire occurrence density mean (fig. 3.8A) and variability (fig. 3.8B) from 2001 through 2021 (17.8 fire occurrences/100 km^2 of tree canopy cover, standard deviation 40.2). This area encompasses recently active portions of the lower east rift zone of Kīlauea volcano, where lava flows from intermittent eruptions have incinerated some forested areas (Andrews 2018). With the exception of the Mesic region on Hawai'i Island

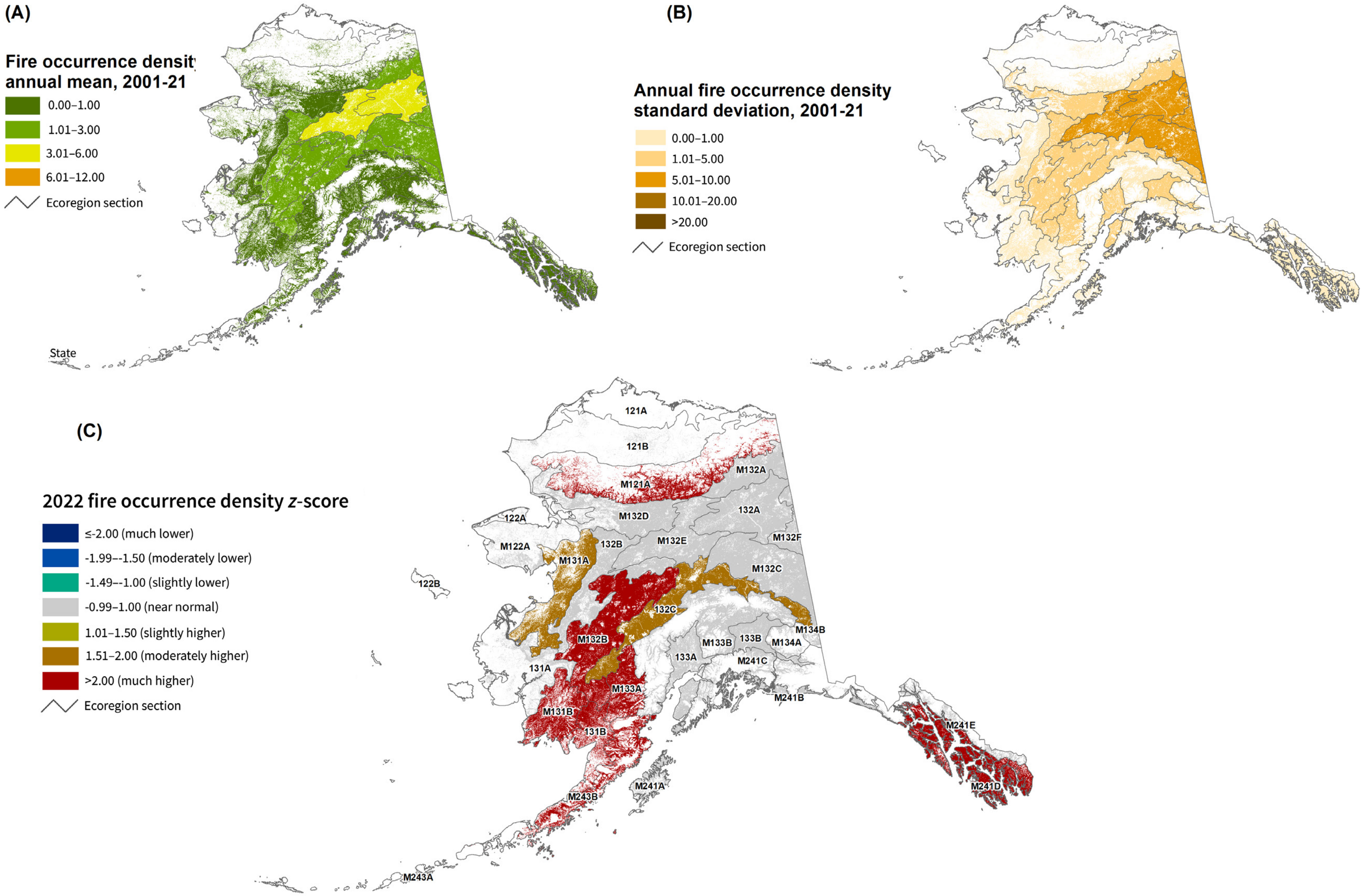

Figure 3.7—(A) Mean number and (B) standard deviation of forest fire occurrences per 100 km² (10 000 ha) of forest and shrub cover from 2001 through 2021, by ecoregion section in Alaska. (C) Degree of 2022 fire occurrence density excess or deficiency, by ecoregion section relative to 2001–2021 and accounting for variation over that period. The gray lines delineate ecoregion sections (Spencer and others 2002). Forest and shrub cover are derived from the 2011 National Land Cover Database. (Source of fire data: U.S. Department of Agriculture, Forest Service, Geospatial Technology and Applications Center, in conjunction with the NASA Moderate Resolution Imaging Spectroradiometer Rapid Response group)

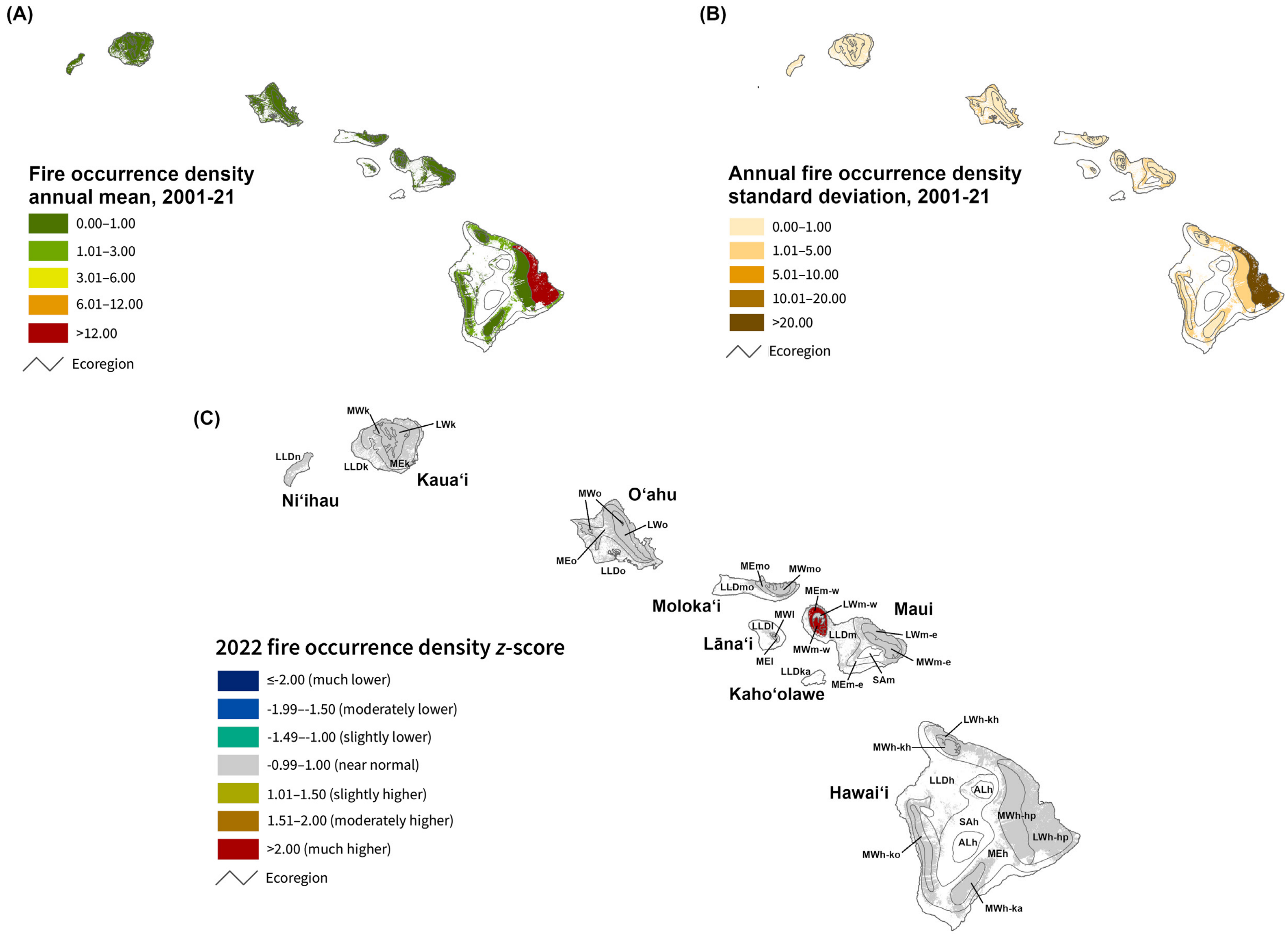

Figure 3.8—(A) Mean number and (B) standard deviation of forest fire occurrences per 100 km^2 (10 000 ha) of tree canopy coverage area from 2001 through 2021, by island/ecoregion combination in Hawaii. (C) Degree of 2022 fire occurrence density excess or deficiency, by island/ecoregion combination relative to 2001–2021 and accounting for variation over that period. Tree canopy cover is based on data from a cooperative project between the Multi-Resolution Land Characteristics Consortium (Coulston and others 2012) and the Forest Service Geospatial Technology and Applications Center (GTAC) using the 2011 National Land Cover Database. (Source of fire data: U.S. Department of Agriculture, Forest Service, GTAC, in conjunction with the NASA Moderate Resolution Imaging Spectroradiometer Rapid Response group)

(MEh) where it was 2.2, all other ecological regions in the State had an annual mean fire occurrence density of ≤1 fire occurrence/100 km^2 of tree cover. In 2022, two ecological regions on Maui (Montane Wet-Maui-West (MWm-w) and Mesic-Maui-West (MEm-w)) had higher-than-expected fire occurrence densities (*z*-score >1), controlling for variability over the previous 21 years (fig. 3.8C).

All the islands encompassed by Puerto Rico and the U.S. Virgin Islands had fire occurrence means and standard deviations ≤1 for 2001–2021 (figs. 3.9A and 3.9B). Only one island, tiny Great Hans Lollik Island north of Saint Thomas in the U.S. Virgin Islands, had a higher-than-expected fire occurrence density in 2022 (*z*-score >1) (fig. 3.9C).

Geographic Hotspots of Fire Occurrence Density

Most of the previous results report on fire occurrence density status and trends at the ecoregion scale. Geographic hotspot analyses using units smaller than ecoregions, meanwhile, can offer additional insights into where fire occurrences are more concentrated than expected by chance during a given year. This approach specifically identifies areas across the CONUS with higher-than-expected fire occurrence densities compared to the entire study region. Unlike the previous 2 years (Potter 2022, 2023), this SASH method did not detect any geographic hotspots of extremely high fire occurrence density (G_i^* >24) in 2022. The West, however, had a handful of hotspots of very high fire occurrence density (G_i^* >12 and ≤24) (fig. 3.10).

One such hotspot was centered on M331F–Southern Parks and Rocky Mountain Range in north-central New Mexico, the region of the human-caused Hermits Peak Fire, the largest wildfire in the State's history (Pietsch and Samenow 2022). It burned 138 295 ha between April and October and cost $330 million to contain (National Interagency Coordination Center 2023). Also within the hotspot area were the Cook Fire (24 022 ha, $13 million) and the Cerro Pelado Fire (18 456 ha, $47 million). Another hotspot of very high fire occurrence density was detected in southwestern New Mexico in M313A–White Mountains-San Francisco Peaks-Mogollon Rim. This is the location of the human-caused Black Fire, the second largest fire in New Mexico history (Javaheri and Chinchar 2022), which scorched 131 578 ha between its May 13 ignition and its November 10 containment and cost $60 million to control (National Interagency Coordination Center 2023).

A hotspot of very high fire occurrence density was located in M332A–Idaho Batholith of central Idaho, where the 52 692-ha Moose Fire cost $98 million to contain between its July 17 human-caused ignition and its November 10 containment (National Interagency Coordination Center 2023). A hotspot of high fire occurrence density (G_i^* >6 and ≤12) was detected immediately to the west in northeastern Oregon (M332G–Blue Mountains), where the lightning-caused Double Creek Fire burned 69 417 ha from August through October, with a containment cost of

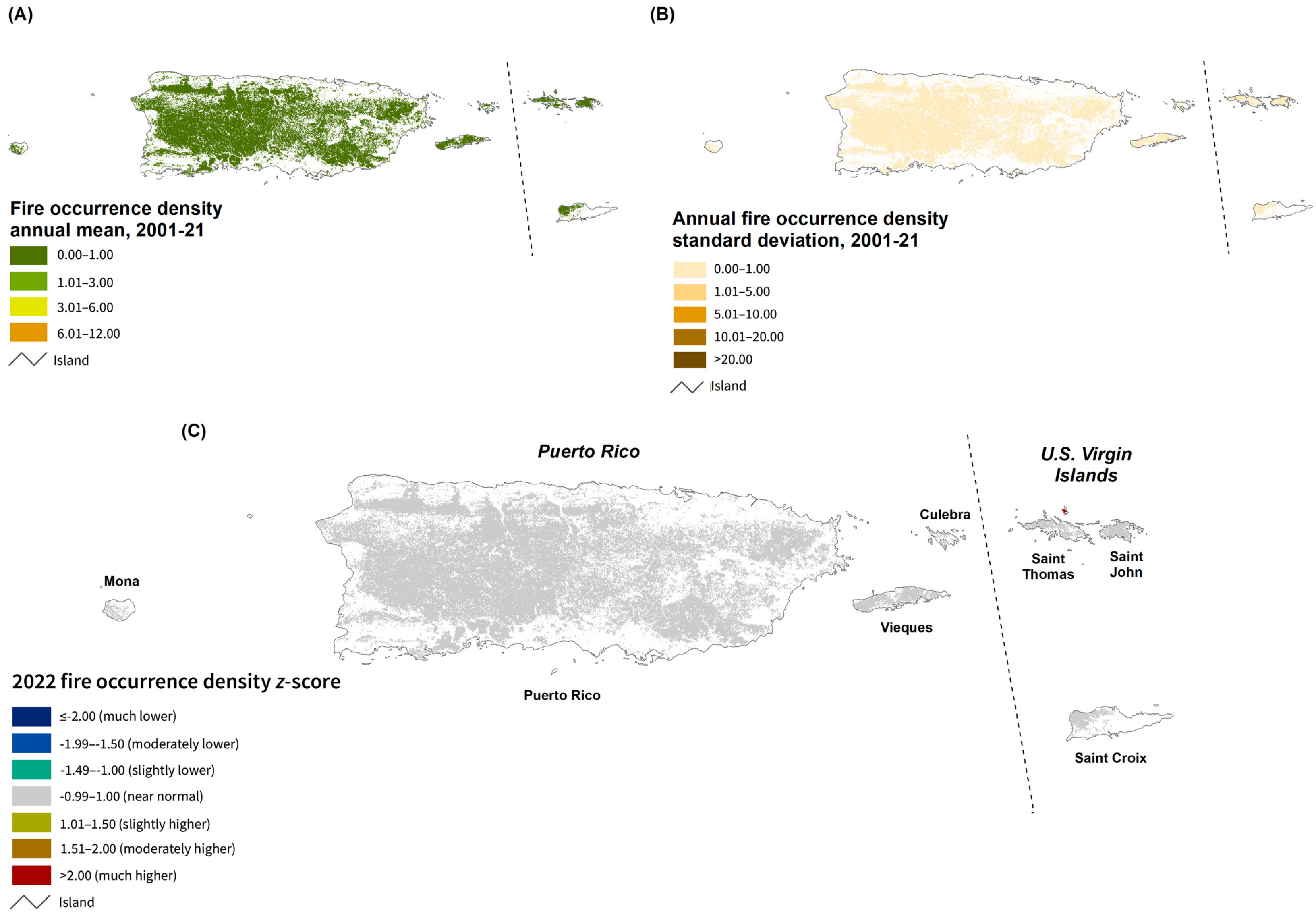

Figure 3.9—(A) Mean number and (B) standard deviation of forest fire occurrences per 100 km² (10 000 ha) of forested area from 2001 through 2021, by island in Puerto Rico and the U.S. Virgin Islands. (C) Degree of 2022 fire occurrence density excess or deficiency, by island relative to 2001–2021 and accounting for variation over that period. Tree canopy cover is based on data from a cooperative project between the Multi-Resolution Land Characteristics Consortium (Coulston and others 2012) and the U.S. Department of Agriculture, Forest Service, Geospatial Technology and Applications Center using the 2011 National Land Cover Database.

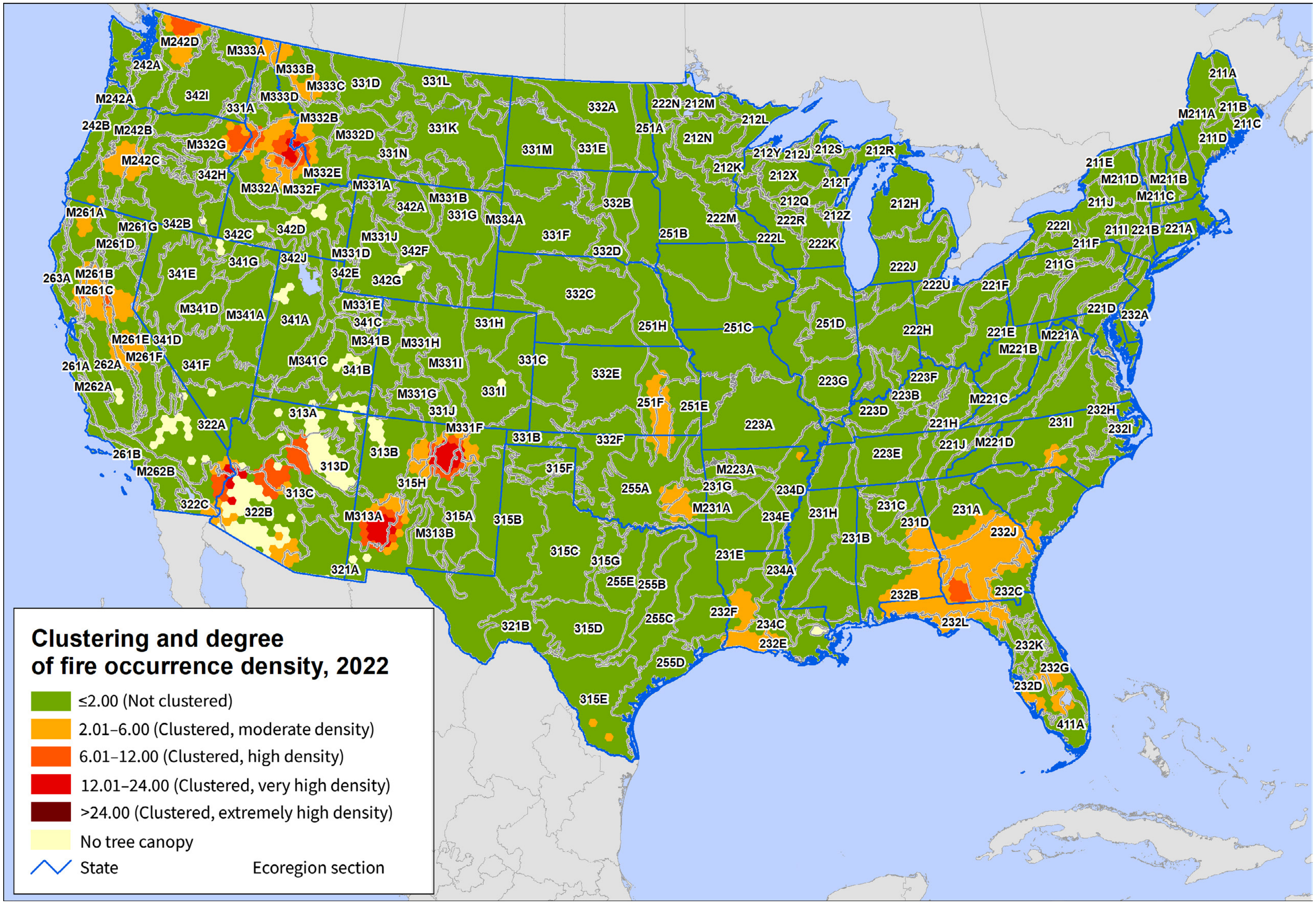

Figure 3.10—Hotspots of fire occurrence, by ecoregion section within the conterminous United States, for 2022. Values are Getis-Ord Gi scores, with values >2 representing significant clustering of high fire occurrence densities. (No areas of significant clustering of lower fire occurrence densities, <-2, were detected.) The gray lines delineate ecoregion sections (Cleland and others 2007).*

$40 million (National Interagency Coordination Center 2023).

Other western hotspots in 2022 included (fig. 3.10):

- Very high occurrence density in an area of sparse forest canopy in southwestern Arizona and southeastern California (322B–Sonoran Desert)
- High occurrence density in central Arizona (313C–Tonto Transition and M313A–White Mountains-San Francisco Peaks-Mogollon Rim)
- High occurrence density in north-central Washington (M242D–Northern Cascades)
- High occurrence density in north-central California (M261E–Sierra Nevada, M261F–Sierra Nevada Foothills, 262A–Great Valley, M261C–Northern California Interior Coast Ranges), location of the $181 million, 31 075-ha Mosquito fire
- Moderate density (G_i^* >2 and ≤6) in west-central Oregon (M242B–Western Cascades and M242B–Western Cascades), site of the $134 million, 51 521-ha Cedar Creek fire

Meanwhile, the SASH analysis detected one high-density and several moderate-density hotspots in the East. The single high-density hotspot was centered on 232B–Gulf Coastal Plains and Flatwoods in southwestern Georgia and extended into neighboring areas as a moderate-density hotspot.

CONCLUSIONS

In 2022, the number of MODIS satellite-detected forest fire occurrences in the CONUS decreased 44 percent from the preceding year, which was the fourth highest in 22 full years of data collection. The 2022 number was also about 17 percent below the annual mean. Despite being a relatively quiet fire year in the CONUS, New Mexico experienced the two largest forest fires in its history and a handful of ecoregions in the Southwest had very high fire occurrence densities (fire occurrences/100 km^2 of tree canopy cover area). Additionally, a handful of ecoregions of the Pacific Northwest and the Southeast experienced high fire occurrence densities. The fire activity in these areas resulted in geographic hotspots of very high or high fire occurrence density. Ecoregions in the Southwest, Northeast, Midwest, and Mid-Atlantic regions experienced fire occurrence densities that were higher than normal in 2022 compared to the previous 21-year mean and accounting for variability over that period. At the same time, a few ecoregion sections in the Southwest and Midwest had significantly lower fire occurrence densities than normal.

Meanwhile, Alaska experienced a 1,000-percent jump in fire occurrences from 2021 to 2022, with the latter year tallying about 140 percent of the mean annual number of fire occurrences across the previous 21 years. This was the result of well-above-normal temperatures through the early summer coupled with lightning-intense storms that sparked a rapid increase in fire activity in June. Ecoregion sections in the central and southwestern part of the State had high fire occurrence densities for 2022, while those ecoregions and others across Alaska—including in the panhandle and far north—had higher-than-expected fire occurrence densities.

Hawaiian forests in 2022 had fire occurrence densities that were low and within expectations, with the exception of two ecological regions on the western part of Maui Island. In the Caribbean, only the tiny island of Great Hans Lollik Island near Saint Thomas in the U.S. Virgin Islands had a higher-than-expected fire occurrence density in 2022.

Rather than quantifying the severity of a given fire season, the results of these geographic analyses offer insights into where fire occurrences were concentrated spatially during a given year and compared to previous years. These products may include commission errors and may underrepresent the number of fire occurrences in some ecosystems where small and low-intensity fires are common in addition to where high cloud frequency can interfere with fire detection. At the same time, these high-temporal-fidelity products currently offer the best means for daily monitoring of forest fire occurrences.

Ecological and forest health impacts relating to fire and other abiotic disturbances are scale-dependent properties, which in turn are affected by management objectives (Lundquist and others 2011). Information about the concentration of fire occurrences may pinpoint areas of concern for aiding management activities and for investigations into the ecological and socioeconomic impacts of forest fire potentially outside the range of historic frequency. Quantifying the location and frequency of forest fire occurrences across the United States also can help to better understand emerging spatiotemporal patterns of fire occurrence in light of climate change and shifting fire regimes.

LITERATURE CITED

Abatzoglou, J.T.; Williams, A.P. 2016. Impact of anthropogenic climate change on wildfire across Western US forests. Proceedings of the National Academy of Sciences. 113(42): 11770–11775. https://doi.org/10.1073/pnas.1607171113.

Agee, J.K. 1998. The landscape ecology of western forest fire regimes. Northwest Science. 72: 24–34.

Andrews, R.G. 2018. America's most hazardous volcano erupted this year. Then it erupted and erupted. The New York Times. December 12. https://www.nytimes.com/2018/12/12/science/kilauea-hawaii-volcano-eruption.html. [Date accessed: July 15, 2019].

Anselin, L. 1992. Spatial data analysis with GIS: an introduction to application in the social sciences. Tech. Rep. 92-10. Santa Barbara, CA: University of California, National Center for Geographic Information and Analysis. 53 p.

Barbour, M.G.; Burk, J.H.; Pitts, W.D. [and others]. 1999. Terrestrial plant ecology. Menlo Park, CA: Addison Wesley Longman, Inc. 649 p.

Bond, W.J.; Keeley, J.E. 2005. Fire as a global "herbivore": the ecology and evolution of flammable ecosystems. Trends in Ecology & Evolution. 20(7): 387–394. https://doi.org/10.1016/j.tree.2005.04.025.

Calkin, D.E.; Thompson, M.P.; Finney, M.A. 2015. Negative consequences of positive feedbacks in US wildfire management. Forest Ecosystems. 2: 9. https://doi.org/10.1186/s40663-015-0033-8.

Cleland, D.T.; Freeouf, J.A.; Keys, J.E. [and others]. 2007. Ecological subregions: sections and subsections for the conterminous United States. Gen. Tech. Rep. WO-76D. Washington, DC: U.S. Department of Agriculture, Forest Service. Map; Sloan, A.M., cartographer; presentation scale 1:3,500,000; colored. https://doi.org/10.2737/WO-GTR-76D.

Coop, J.D.; Parks, S.A.; Stevens-Rumann, C.S. [and others]. 2020. Wildfire-driven forest conversion in western North American landscapes. BioScience. 70(8): 659–673. https://doi.org/10.1093/biosci/biaa061.

Coulston, J.W.; Ambrose, M.J.; Riitters, K.H.; Conkling, B.L. 2005. Forest Health Monitoring 2004 national technical report. Gen. Tech. Rep. SRS-90. Asheville, NC: U.S. Department of Agriculture, Forest Service, Southern Research Station. 81 p. https://doi.org/10.2737/SRS-GTR-90.

Coulston, J.W.; Moisen, G.G.; Wilson, B.T. [and others]. 2012. Modeling percent tree canopy cover: a pilot study. Photogrammetric Engineering and Remote Sensing. 78(7): 715–727. https://doi.org/10.14358/PERS.78.7.715.

Davis, K.T.; Dobrowski, S.Z.; Higuera, P.E.; Maneta, M.P. 2019. Wildfires and climate change push low-elevation forests across critical climate threshold for tree regeneration. Proceedings of the National Academy of Sciences. 116(13): 6193–6198. https://doi.org/10.1073/pnas.181510711.

Edmonds, R.L.; Agee, J.K.; Gara, R.I. 2011. Forest health and protection. Long Grove, IL: Waveland Press, Inc. 667 p.

Eidenshink, J.; Schwind, B.; Brewer, K. [and others]. 2007. A project for monitoring trends in burn severity. Fire Ecology. 3(1): 3–21. https://doi.org/10.4996/fireecology.0301003.

ESRI. 2017. ArcMap® 10.5.1. Redlands, CA: Environmental Systems Research Institute.

Getis, A.; Ord, J.K. 1992. The analysis of spatial association by use of distance statistics. Geographical Analysis. 24(3): 189–206. https://doi.org/10.1111/j.1538-4632.1992.tb00261.x.

Giglio, L.; Descloitres, J.; Justice, C.O.; Kaufman, Y.J. 2003. An enhanced contextual fire detection algorithm for MODIS. Remote Sensing of Environment. 87(2–3): 273–282. https://doi.org/10.1016/S0034-4257(03)00184-6.

Giglio, L.; Schroeder, W.; Hall, J.V.; Justice, C.O. 2018. MODIS Collection 6 active fire product user's guide: revision B. https://cdn.earthdata.nasa.gov/conduit/upload/10575/MODIS_C6_Fire_User_Guide_B.pdf. [Date accessed: May 16, 2022].

Gill, A.M.; Stephens, S.L.; Cary, G.J. 2013. The worldwide "wildfire" problem. Ecological Applications. 23(2): 438–454. https://doi.org/10.1890/10-2213.1.

Greenberg, C.H.; Collins, B., eds. 2021. Fire ecology and management across U.S. forests: past, present, and future. Cham, Switzerland: Springer. 502 p.

Hanberry, B.B.; Bragg, D.C.; Hutchinson, T.F. 2018. A reconceptualization of open oak and pine ecosystems of eastern North America using a forest structure spectrum. Ecosphere. 9(10): e02431. https://doi.org/10.1002/ecs2.2431.

Hawbaker, T.J.; Radeloff, V.C.; Syphard, A.D. [and others]. 2008. Detection rates of the MODIS active fire product. Remote Sensing of Environment. 112: 2656–2664. https://doi.org/10.1016/j.rse.2007.12.008.

Higuera, P.E.; Abatzoglou, J.T. 2021. Record-setting climate enabled the extraordinary 2020 fire season in the western United States. Global Change Biology. 27(1). https://doi.org/10.1111/gcb.15388.

Homer, C.G.; Dewitz, J.A.; Yang, L. [and others]. 2015. Completion of the 2011 National Land Cover Database for the conterminous United States: representing a decade of land cover change information. Photogrammetric Engineering and Remote Sensing. 81(5): 345–354.

Javaheri, P.; Chinchar, A. 2022. Black Fire becomes New Mexico's 2nd largest fire in the state's history. CNN. June 10. https://www.cnn.com/2022/06/09/weather/historic-simultaneous-new-mexico-wildfires-weekend/index.html. [Date accessed: April 20, 2013].

Jeronimo, S.M.; Kane, V.R.; Churchill, D.J. [and others]. 2019. Forest structure and pattern vary by climate and landform across active-fire landscapes in the montane Sierra Nevada. Forest Ecology and Management. 437: 70–86. https://doi.org/10.1016/j.foreco.2019.01.033.

Justice, C.O.; Giglio, L.; Korontzi, S. [and others]. 2002. The MODIS fire products. Remote Sensing of Environment. 83(1–2): 244–262. https://doi.org/10.1016/S0034-4257(02)00076-7.

Justice, C.O.; Giglio, L.; Roy, D. [and others]. 2011. MODIS-derived global fire products. In: Ramachandran, B.; Justice, C.O.; Abrams, M.J., eds. Land remote sensing and global environmental change: NASA's earth observing system and the science of ASTER and MODIS. New York: Springer: 661–679. https://doi.org/10.1007/978-1-4419-6749-7_29.

Kiser, D.; Elhanan, G.; Metcalf, W.J. [and others]. 2021. SARS-CoV-2 test positivity rate in Reno, Nevada: association with PM2.5 during the 2020 wildfire smoke events in the Western United States. Journal of Exposure Science and Environmental Epidemiology. 31: 797–803. https://doi.org/10.1038/s41370-021-00366-w.

Laffan, S.W. 2006. Assessing regional scale weed distributions, with an Australian example using *Nassella trichotoma*. Weed Research. 46(3): 194–206. https://doi.org/10.1111/j.1365-3180.2006.00491.x.

Lundquist, J.E.; Camp, A.E.; Tyrrell, M.L. [and others]. 2011. Earth, wind and fire: abiotic factors and the impacts of global environmental change on forest health. In: Castello, J.D.; Teale, S.A., eds. Forest health: an integrated perspective. New York: Cambridge University Press: 195–243. https://doi.org/10.1017/CBO9780511974977.008.

May, C.J.; Zald, H.S.J.; North, M.P. [and others]. 2023. Repeated burns fail to restore pine regeneration to the natural range of variability in a Sierra Nevada mixed-conifer forest, U.S.A. Restoration Ecology. e13863. https://doi.org/10.1111/rec.13863.

NASA Fire Information for Resource Management System. 2022. FIRMS frequently asked questions. https://earthdata.nasa.gov/faq/firms-faq. [Date accessed: May 16, 2022].

NASA Fire Information for Resource Management System. 2023. MODIS fire archive download tool. https://firms.modaps.eosdis.nasa.gov/download/. [Date accessed: April 11, 2023].

National Interagency Coordination Center. 2021. Wildland fire summary and statistics annual report: 2020. https://www.nifc.gov/sites/default/files/NICC/2-Predictive%20Services/Intelligence/Annual%20Reports/2020/annual_report_0.pdf. [Date accessed: November 06, 2024].

National Interagency Coordination Center. 2022. Wildland fire summary and statistics annual report: 2021. https://www.nifc.gov/sites/default/files/NICC/2-Predictive%20Services/Intelligence/Annual%20Reports/2021/annual_report_0.pdf. [Date accessed: November 6, 2024].

National Interagency Coordination Center. 2023. Wildland fire summary and statistics annual report: 2022. https://www.nifc.gov/sites/default/files/NICC/2-Predictive%20Services/Intelligence/Annual%20Reports/2022/annual_report.2.pdf. [Date accessed: November 06, 2024].

Nowacki, G.J.; Abrams, M.D. 2008. The demise of fire and "mesophication" of forests in the Eastern United States. BioScience. 58(2): 123–138. https://doi.org/10.1641/B580207.

Nowell, H.K.; Holmes, C.D.; Robertson, K. [and others]. 2018. A new picture of fire extent, variability, and drought interaction in prescribed fire landscapes: insights from Florida government records. Geophysical Research Letters. 45(15): 7874–7884. https://doi.org/10.1029/2018GL078679.

Parisien, M.A.; Miller, C.; Parks, S.A. [and others]. 2016. The spatially varying influence of humans on fire probability in North America. Environmental Research Letters. 11(7): 1–18. https://doi.org/10.1088/1748-9326/11/7/075005.

Pausas, J.G.; Keeley, J.E. 2019. Wildfires as an ecosystem service. Frontiers in Ecology and the Environment. 17(5): 289–295. https://doi.org/10.1002/fee.2044.

Picotte, J.J.; Bhattarai, K.; Howard, D. [and others]. 2020. Changes to the Monitoring Trends in Burn Severity program mapping production procedures and data products. Fire Ecology. 16: 16. https://doi.org/10.1186/s42408-020-00076-y.

Pietch, B.; Samenow, J. 2022. New Mexico blaze is now largest wildfire in state history. The Washington Post. May 17. https://www.washingtonpost.com/nation/2022/05/17/calf-canyon-hermits-peak-fire-new-mexico/. [Date accessed: April 19, 2023].

Potter, K.M. 2012a. Large-scale patterns of forest fire occurrence in the conterminous United States and Alaska, 2005–07. In: Potter, K.M.; Conkling, B.L., eds. Forest Health Monitoring 2008 national technical report. Gen. Tech. Rep. SRS-158. Asheville, NC: U.S. Department of Agriculture, Forest Service, Southern Research Station: 73–83.

Potter, K.M. 2012b. Large-scale patterns of forest fire occurrence in the conterminous United States and Alaska, 2001–08. In: Potter, K.M.; Conkling, B.L., eds. Forest Health Monitoring 2009 national technical report. Gen. Tech. Rep. SRS-167. Asheville, NC: U.S. Department of Agriculture, Forest Service, Southern Research Station: 151–161.

Potter, K.M. 2013a. Large-scale patterns of forest fire occurrence in the conterminous United States and Alaska, 2009. In: Potter, K.M.; Conkling, B.L., eds. Forest Health Monitoring: national status, trends, and analysis 2010. Gen. Tech. Rep. SRS-176. Asheville, NC: U.S. Department of Agriculture, Forest Service, Southern Research Station: 31–39.

Potter, K.M. 2013b. Large-scale patterns of forest fire occurrence in the conterminous United States and Alaska, 2010. In: Potter, K.M.; Conkling, B.L., eds. Forest Health Monitoring: national status, trends, and analysis 2011. Gen. Tech. Rep. SRS-185. Asheville, NC: U.S. Department of Agriculture, Forest Service, Southern Research Station: 29–40.

Potter, K.M. 2014. Large-scale patterns of forest fire occurrence in the conterminous United States and Alaska, 2011. In: Potter, K.M.; Conkling, B.L., eds. Forest Health Monitoring: national status, trends, and analysis 2012. Gen. Tech. Rep. SRS-198. Asheville, NC: U.S. Department of Agriculture, Forest Service, Southern Research Station: 35–48.

Potter, K.M. 2015a. Large-scale patterns of forest fire occurrence in the conterminous United States and Alaska, 2012. In: Potter, K.M.; Conkling, B.L., eds. Forest Health Monitoring: national status, trends, and analysis 2013. Gen. Tech. Rep. SRS-207. Asheville, NC: U.S. Department of Agriculture, Forest Service, Southern Research Station: 37–53.

Potter, K.M. 2015b. Large-scale patterns of forest fire occurrence in the conterminous United States and Alaska, 2013. In: Potter, K.M.; Conkling, B.L., eds. Forest Health Monitoring: national status, trends, and analysis 2014. Gen. Tech. Rep. SRS-209. Asheville, NC: U.S. Department of Agriculture, Forest Service, Southern Research Station: 39–55.

Potter, K.M. 2016. Large-scale patterns of forest fire occurrence in the conterminous United States, Alaska, and Hawaii, 2014. In: Potter, K.M.; Conkling, B.L., eds. Forest Health Monitoring: national status, trends, and analysis 2015. Gen. Tech. Rep. SRS-213. Asheville, NC: U.S. Department of Agriculture, Forest Service, Southern Research Station: 41–60.

Potter, K.M. 2017. Large-scale patterns of forest fire occurrence in the conterminous United States, Alaska, and Hawaii, 2015. In: Potter, K.M.; Conkling, B.L., eds. Forest Health Monitoring: national status, trends, and analysis 2016. Gen. Tech. Rep. SRS-222. Asheville, NC: U.S. Department of Agriculture, Forest Service, Southern Research Station: 43–62.

Potter, K.M. 2018. Large-scale patterns of forest fire occurrence in the conterminous United States, Alaska, and Hawaii, 2016. In: Potter, K.M.; Conkling, B.L., eds. Forest Health Monitoring: national status, trends, and analysis 2017. Gen. Tech. Rep. SRS-233. Asheville, NC: U.S. Department of Agriculture, Forest Service, Southern Research Station: 45–64.

Potter, K.M. 2019. Large-scale patterns of forest fire occurrence across the 50 United States and the Caribbean territories, 2017. In: Potter, K.M.; Conkling, B.L., eds. Forest Health Monitoring: national status, trends, and analysis 2018. Gen. Tech. Rep. SRS-239. Asheville, NC: U.S. Department of Agriculture, Forest Service, Southern Research Station: 51–76.

Potter, K.M. 2020a. Large-scale patterns of forest fire occurrence across the 50 United States and the Caribbean territories, 2018. In: Potter, K.M.; Conkling, B.L., eds. Forest Health Monitoring: national status, trends, and analysis 2019. Gen. Tech. Rep. SRS-250. Asheville, NC: U.S. Department of Agriculture, Forest Service, Southern Research Station: 57–82.

Potter, K.M. 2020b. Introduction. In: Potter, K.M.; Conkling, B.L., eds. Forest Health Monitoring: national status, trends, and analysis 2019. Gen. Tech. Rep. SRS-250. Asheville, NC: U.S. Department of Agriculture, Forest Service, Southern Research Station: 5–24.

Potter, K.M. 2021. Broad-scale patterns of forest fire occurrence across the 50 United States and the Caribbean territories, 2019. In: Potter, K.M.; Conkling, B.L., eds. Forest Health Monitoring: national status, trends, and analysis 2020. Gen. Tech. Rep. SRS-261. Asheville, NC: U.S. Department of Agriculture, Forest Service, Southern Research Station: 59–84.

Potter, K.M. 2022. Broad-scale patterns of forest fire occurrence across the 50 United States and the Caribbean territories, 2020. In: Potter, K.M.; Conkling, B.L., eds. Forest Health Monitoring: national status, trends, and analysis 2021. Gen. Tech. Rep. SRS-266. Asheville, NC: U.S. Department of Agriculture, Forest Service, Southern Research Station: 51–78. https://doi.org/10.2737/SRS-GTR-266-Chap3.

Potter, K.M. 2023. Broad-scale patterns of forest fire occurrence across the United States and the Caribbean territories, 2021. In: Potter, K.M.; Conkling, B.L., eds. Forest Health Monitoring: national status, trends, and analysis 2022. Gen. Tech. Rep. SRS-273. Asheville, NC: U.S. Department of Agriculture, Forest Service, Southern Research Station: 55–81. https://doi.org/10.2737/SRS-GTR-273-Chap3.

Potter, K.M.; Koch, F.H.; Oswalt, C.M.; Iannone, B.V. 2016. Data, data everywhere: detecting spatial patterns in fine-scale ecological information collected across a continent. Landscape Ecology. 31: 67–84. https://doi.org/10.1007/s10980-015-0295-0.

Pyne, S.J. 2010. America's fires: a historical context for policy and practice. Durham, NC: Forest History Society. 91 p.

Radeloff, V.C.; Helmers, D.P.; Anu Kramer, H. [and others]. 2018. Rapid growth of the US wildland-urban interface raises wildfire risk. Proceedings of the National Academy of Sciences. 115(13): 3314–3319. https://doi.org/10.1073/pnas.1718850115.

Reams, G.A.; Smith, W.D.; Hansen, M.H. [and others]. 2005. The Forest Inventory and Analysis sampling frame. In: Bechtold, W.A.; Patterson, P.L., eds. The enhanced Forest Inventory and Analysis Program—national sampling design and estimation procedures. Gen. Tech. Rep. SRS-80. Asheville, NC: U.S. Department of Agriculture, Forest Service, Southern Research Station: 11–26.

Richardson, L.A.; Champ, P.A.; Loomis, J.B. 2012. The hidden cost of wildfires: economic valuation of health effects of wildfire smoke exposure in southern California. Journal of Forest Economics. 18(1): 14–35. https://doi.org/10.1016/j.jfe.2011.05.002.

Schmidt, K.M.; Menakis, J.P.; Hardy, C.C. [and others]. 2002. Development of coarse-scale spatial data for wildland fire and fuel management. Gen. Tech. Rep. RMRS-87. Fort Collins, CO: U.S. Department of Agriculture, Forest Service, Rocky Mountain Research Station. 41 p. https://doi.org/10.2737/RMRS-GTR-87.

Shima, T.; Sugimoto, S.; Okutomi, M. 2010. Comparison of image alignment on hexagonal and square lattices. In: 2010 IEEE international conference on image processing. [Place of publication unknown]: Institute of Electrical and Electronics Engineers, Inc.: 141–144. https://doi.org/10.1109/ICIP.2010.5654351.

Spencer, P.; Nowacki, G.; Fleming, M. [and others]. 2002. Home is where the habitat is: an ecosystem foundation for wildlife distribution and behavior. Arctic Research of the United States. 16: 6–17.

Stephens, S.L.; Collins, B.M.; Fettig, C.J. [and others]. 2018. Drought, tree mortality, and wildfire in forests adapted to frequent fire. BioScience. 68(2): 77–88. https://doi.org/10.1093/biosci/bix146.

Thom, D.; Seidl, R. 2016. Natural disturbance impacts on ecosystem services and biodiversity in temperate and boreal forests. Biological Reviews. 91(3): 760–781. https://doi.org/10.1111/brv.12193.

Tonini, M.; Tuia, D.; Ratle, F. 2009. Detection of clusters using space-time scan statistics. International Journal of Wildland Fire. 18(7): 830–836. https://doi.org/10.1071/WF07167.

Wade, D.D.; Brock, B.L.; Brose, P. [and others]. 2000. Fire in eastern ecosystems. In: Brown, J.K.; Kapler, J., eds. Wildland fire in ecosystems: effects of fire on flora. Gen. Tech. Rep. RMRS-42-vol. 2. Ogden, UT: U.S. Department of Agriculture, Forest Service, Rocky Mountain Research Station: 53–96.

White, D.; Kimerling, A.J.; Overton, W.S. 1992. Cartographic and geometric components of a global sampling design for environmental monitoring. Cartography and Geographic Information Systems. 19(1): 5–22. https://doi.org/10.1559/152304092783786636.